Measurement of neutron-capture cross sections of ^{70,72}Ge using the DANCE facility

A. Laminack,[1,2] J. C. Blackmon,[1] A. Couture,[3] J. P. Greene,[4] M. Krtička,[5] K. T. Macon,[6,*] S. Mosby,[3] C. Prokop,[3] J. L. Ullmann,[3] and S. Valenta[5]

[1]*Louisiana State University, Baton Rouge, Louisiana 70803, USA*
[2]*Physics Division, Oak Ridge National Laboratory, Oak Ridge, Tennessee 37831, USA*
[3]*Los Alamos National Laboratory, Los Alamos, New Mexico 87545, USA*
[4]*Argonne National Laboratory, 9700 South Cass Avenue, Argonne, Illinois 60439, USA*
[5]*Charles University, Faculty of Mathematics and Physics, Prague, Czech Republic*
[6]*University of Notre Dame, Notre Dame, Indiana 46556, USA*

(Received 13 May 2022; accepted 26 July 2022; published 3 August 2022)

Background: Approximately half of all atomic nuclei heavier than iron are synthesized by the slow neutron-capture process. The weak component of this process is not well understood and the reaction rates of each isotope in the s-process path affect nucleosynthesis abundances downstream.
Purpose: To measure the neutron-capture cross sections of two weak s-process nuclei, ^{70,72}Ge, using the neutron time-of-flight technique. Measuring the capture cross sections for isotopes in this region of the chart of nuclides has proven challenging due to dominant scattering cross sections.
Method: Samples consisted of pellets made of pressed enriched metallic powders. The ^{70,72}Ge neutron-capture cross sections were measured as a function of neutron energy using the Detector for Advanced Neutron Capture Experiments at Los Alamos National Laboratory.
Results: Neutron-capture cross sections were measured from 10 eV to 1 MeV. These are the first measurements for ^{70,72}Ge between 300 keV and 1 MeV neutron energy. Maxwellian-averaged cross sections were calculated in the astrophysically relevant neutron energy range (5 keV $\leqslant kT \leqslant$ 100 keV). Their value at $kT = 30$ keV was found to be 89 ± 11 mb for ^{70}Ge and 58 ± 5 mb for ^{72}Ge. Both values are in agreement with recent time-of-flight measurements at n_TOF (neutron Time-Of-Flight facility at the European Organization for Nuclear Research).
Conclusions: The average cross section results from this work for ^{70}Ge show minor ($<1\sigma$) disagreement with a recent measurement by the n_TOF collaboration at higher neutron energies. This corresponds to the neutron energy region that had previously never been measured (>300 keV). Two reaction library databases underestimate the ^{72}Ge average cross section below 30 keV according to n_TOF and DANCE. This is likely due to capture resonances that are missing from the theoretical cross sections in the databases that were identified in both time-of-flight measurements. Additionally, a rudimentary analysis of the impact of both cross section measurements on stellar nucleosynthesis abundances using the NETZ nucleosynthesis tool is presented.

DOI: 10.1103/PhysRevC.106.025802

I. INTRODUCTION

The slow neutron-capture process (s process) is responsible for synthesizing roughly half of all atomic nuclei heavier than iron [1]. The s process can be further divided into two parts: the main component and the weak component [2,3]. In heavy (8–25 $M_\odot$) main sequence stars, the weak component of the s process synthesizes elements up to strontium or yttrium ($A = 88, 89$). Studies have been carried out to investigate how sensitive the s-process isotopic abundances are to changes in reaction rates of other isotopes in the s-process path [4,5]. The results show that changes in the reaction rates of lighter weak s-process nuclei have a downstream effect on heavier isotopes and cause significant changes in isotopic abundances [5]. This is because the weak s process occurs in a low neutron density environment. Therefore, an accurate measure of the radiative neutron capture cross sections of s-process elements is critical to understanding isotopic abundances in the weak s-process. Measuring these cross sections has proven to be challenging as they are generally much smaller than the scattering cross sections in this region of the chart of nuclides.

All stable germanium isotopes (^{70,72,73,74,76}Ge) participate in the weak s process, but ^{72}Ge was identified by Pignatari *et al.* as being of particular importance [5]. Additionally, ^{70}Ge is one of the few s-only isotopes in the weak s process, making it an important isotope for constraining s-process abundances [6].

There are few experimental measurements of the ^{70,72}Ge radiative neutron capture cross sections. Both isotopes were recently measured by the neutron Time-Of-Flight (n_TOF) collaboration [7,8]. ^{70}Ge had been measured previously only one time by Walter and Beer in 1985 [9], and ^{72}Ge had never been measured before the n_TOF measurement. Given the

[*]Present address: InstroTek®, 1 Triangle Dr., Research Triangle Park, NC 27709, USA.

TABLE I. The isotopic composition of the five germanium samples. Bold numbers indicate the enrichment of the target isotope in each sample.

Sample	Mass (mg)	Isotopic abundance (%)				
		^{70}Ge	^{72}Ge	^{73}Ge	^{74}Ge	^{76}Ge
^{70}Ge	97.6	**95.85**	4.09	0.04	0.02	
^{72}Ge	108.4	0.29	**98.2**	0.29	1.04	0.18
^{73}Ge	76.5	0.005	1.36	**96.34**	2.29	0.005
^{74}Ge	207.6	0.01	0.16	1.9	**97.53**	0.4
^{76}Ge	265.8	0.004	0.009	0.028	12.68	**88.1**

dearth of measurements for these isotopes, additional measurements to validate the recent n_TOF results are necessary.

The neutron-capture cross sections of ^{70,72,74,76}Ge were measured via the neutron time-of-flight method at Los Alamos National Laboratory. Presented in this paper are the results from the measurement of ^{70,72}Ge. The results for ^{74,76}Ge will be presented in a forthcoming paper as there is additional motivation for their measurement.

II. EXPERIMENTAL TECHNIQUE

Measurements were conducted at the Los Alamos Neutron Science Center (LANSCE) at Los Alamos National Laboratory (LANL). At LANSCE, an 800-MeV proton beam is produced using a linear accelerator. This beam is bunched into pulses using a proton storage ring before being delivered to a tungsten target where neutrons are produced by high-energy spallation reactions. The neutrons are moderated by a water moderator before traveling down flight path 14 and impinging on a sample located at a flight path length of 20.3 m [10]. Neutron energies are determined via the time of flight.

Surrounding the sample is an array of 160 BaF_2 detectors that form the Detector for Advanced Neutron Capture Experiments (DANCE), a nearly 4π solid angle calorimeter [11]. The high timing resolution of BaF_2 permits a narrow coincidence window, reducing effects from multiple event detection.

Two beam monitors are placed downstream from DANCE to determine the neutron flux at the sample location: a ^{6}LiF converter foil coupled to a silicon detector and a ^{235}U fission chamber. Due to the respective reaction cross sections, each of these detectors are properly equipped to handle different neutron energy regimes: ^{6}LiF for $E_n \leqslant 5$ keV and ^{235}U for $E_n \geqslant 5$ keV. The yield of the ^{235}U fission counter is normalized to that of the ^{6}Li detector from 3 to 5 keV neutron energy where both cross sections are smoothly varying. This normalization accounts for any detector geometry effects such as solid angle coverage so that a consistent flux can be determined.

Several samples were used during the experimental campaign. Highly enriched samples of each germanium isotope, a lead sample that reproduces the effects of neutron scattering, and a gold sample with a thickness of 5 kÅ for flux normalization were used. The isotopic assays and masses for the germanium targets are shown in Table I. Most of the germanium samples were delivered by trace isotopes in the form of a metallic powder. The powder was pressed into cylinders with a diameter of approximately 5 mm. The lone exception is the ^{76}Ge sample which was provided by the LEGEND collaboration [12].

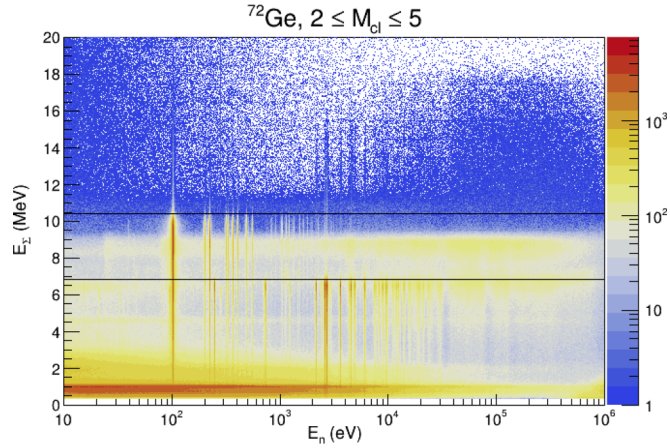

FIG. 1. The E_Σ vs E_n spectrum for cluster multiplicities $M_{cl} =$ 2–5 from ^{72}Ge. Note the different line lengths in E_Σ indicating different reaction Q values from different isotopes in the target. Horizontal lines at 6.78 and 10.2 MeV have been placed to denote the S_n of ^{72}Ge and ^{73}Ge, respectively.

III. DATA ANALYSIS

A. Background subtraction

All DANCE detectors firing within the 10-ns coincidence window are considered to have detected γ rays from a single neutron capture. Several observables are available for each capture event. The most important ones are neutron energy (E_n), sum of γ-ray energies detected by DANCE (E_Σ), and γ-ray multiplicity. When γ rays are detected in a BaF_2 crystal, they often scatter into a neighboring crystal. Neighboring crystals that fire within the coincidence window are grouped together as a cluster. The cluster multiplicity (M_{cl}) is used as a proxy for γ-ray multiplicity. For a chosen set of M_{cl}, a spectrum of E_Σ as a function of E_n is then constructed. Only the fraction of events with $M_{cl} =$ 2–5 are included in the analysis since $M_{cl} = 1$ is strongly dominated by backgrounds including neutron scattering and there are few events with $M_{cl} > 5$. An example of the E_Σ vs E_n spectrum for ^{72}Ge is shown in Fig. 1. This spectrum illustrates the strength of DANCE as a calorimeter. The capture events form a peak near the reaction Q value, corresponding to a complete detection of emitted γ rays and a tail toward to lower energies formed by events where a fraction of emitted γ-ray energy escapes detection. Pile-up from detection of γ rays from multiple captures can be seen for strong resonances, though this is a negligible portion of events because of the narrow coincidence window.

The E_Σ spectrum is composed of captures on the isotopes of interest as well as contaminant Ge isotopes, captures of scattered neutrons in Ba present in detectors, beam-on backgrounds (more detail later), and a beam-off, ambient background. Beam-off background events are primarily low E_Σ and single cluster multiplicity. Since both of these regions

TABLE II. Neutron separation energies S_n for stable germanium isotopes.

Isotope	^{70}Ge	^{72}Ge	^{73}Ge	^{74}Ge	^{76}Ge
S_n (MeV)	7.42	6.78	10.20	6.51	6.07

are excluded in the analysis, they are neglected. In order to subtract the dominant backgrounds leaving only the yield from the isotope of interest, the calorimetric properties of DANCE are exploited. Since γ cascades produce peaks in E_Σ near the capture Q value, the signatures of each isotope can be differentiated based on the Q value of the reaction. The Q value for neutron capture is the neutron separation energy plus the incident neutron energy. The neutron separation energies for each stable germanium isotope are shown in Table II.

The reaction with the highest Q value will produce a spectrum in E_Σ whose peak is higher in energy than all others. In all of the germanium samples, this background comes from neutron captures on ^{73}Ge. By going bin by bin in neutron energy and projecting onto the E_Σ axis, an E_Σ profile at individual neutron energies is acquired. The amount of ^{73}Ge to be subtracted within that E_n bin is identified by matching the portion of the E_Σ spectrum that occurs above the Q values from all other reactions. This range for ^{73}Ge is between 9.6 and 10.2 MeV. The bin-by-bin background subtraction procedure is preferred in the case that neutron energy spectra are not consistent between samples. This technique is even more important in the case of background from scattered neutrons where the scattering cross section of the germanium samples and the lead sample have a different neutron energy dependence.

Next, contributions from neutron scattering are subtracted. Scattered neutrons are captured by barium isotopes in the BaF_2 detectors and the ensuing γ cascades are detected. The stable barium isotopes in the detectors of DANCE are ^{134,135,136,137,138}Ba and have neutron separation energies of 6.97, 9.11, 6.90, 8.61, and 4.72 MeV, respectively. Since the capture Q values for ^{135,137}Ba are above the capture Q value for ^{70,72}Ge, the scattering contribution can be subtracted in a similar fashion to ^{73}Ge by normalizing the lead target scattering data to the peak above the ^{70,72}Ge Q values. For ^{70,72}Ge, the spectra were matched from 7.8 to 9.1 MeV. An example of this process is shown in Fig. 2 for $E_n = 94$–95 eV.

While lead accurately reproduces the E_Σ spectrum from neutron scattering above about 4.5 MeV, there is an important discrepancy to note at lower E_Σ. Neutron captures on ^{1}H in the water moderator at LANSCE produce a 2.2-MeV γ-ray component to the beam. Since lead has a significantly higher Z than germanium, the lead target scatters more of these γ rays into the crystals of DANCE than the germanium targets do. Additionally, pair production resulting in two back-to-back 511-keV photons shows up in both E_Σ spectra. Again, the higher Z of lead results in a higher cross section for pair production and thus an enhancement in the E_Σ spectrum around 1 MeV. Because of these issues with the background subtraction, the low E_Σ and $M_{\rm cl} = 1$ data will be excluded

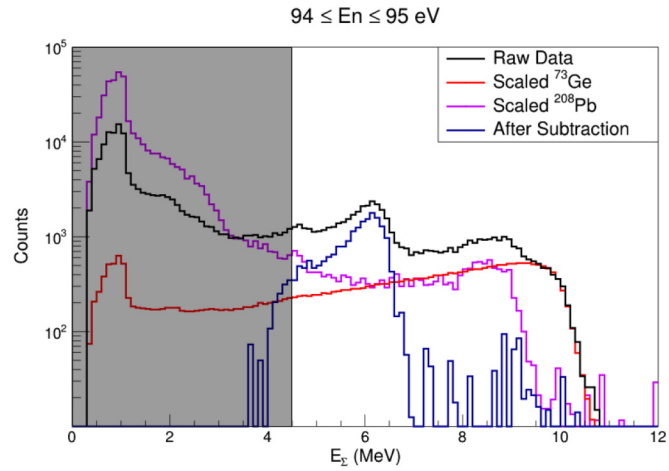

FIG. 2. An example of a E_Σ spectrum from the ^{72}Ge target data at $E_n = 94$–95 eV and $M_{\rm cl} = 2$–5. This shows the raw data (black), the scaled E_Σ spectrum from capture on ^{73}Ge (red), the scaled scattering spectrum (magenta), and the results of the ^{73}Ge and scattering subtraction (blue). The scattering subtraction is unrealistic below about 4.5 MeV so the shaded region is excluded from the yield calculation (see text for details).

when the capture yield is determined. Accounting for this exclusion will be discussed in a later section of the paper.

Finally, contributions from other germanium isotopes with similar Q value to the isotope of interest must be subtracted. The normalization technique described above cannot be used since Q-value peaks separated by about 500 keV or less cannot be sufficiently resolved. Instead, the ^{73}Ge and scattering backgrounds were subtracted from each of the parasitic germanium target spectra. These background-subtracted spectra are normalized using a strong, isolated resonance of the parasitic germanium isotope.

The entire E_Σ vs E_n spectrum corresponding to the parasitic isotope is then subtracted from that of the isotopes of interest using a single normalization factor. The ideal ^{70}Ge resonance that appears in the ^{72}Ge sample is near 1474-eV neutron energy. The cross sections multiplied by the relative abundances for ^{70,72}Ge in the ^{72}Ge sample result in a ratio of approximately 400:1 in this region favoring ^{70}Ge. For the ^{70}Ge sample, the ^{72}Ge resonance at 1118-eV neutron energy is used for normalization. There is approximately a 2900:1 ratio favoring ^{72}Ge in this neutron energy region. Additionally, the ^{74}Ge background is subtracted from the ^{72}Ge data by gating on the resonance near 3051 eV. This resonance favors ^{74}Ge in the ^{72}Ge sample by a factor of about 500.

B. Neutron fluence determination

Directly measuring the fluence at the target location is challenging. Instead, the yield of the beam monitor, $Y_{\rm BM}$, is measured as a function of E_n and divided by the relevant detection cross section, $\sigma_{\rm BM}$, for the beam monitor. This quantity is proportional to the neutron fluence, Φ_T, at the target location and does not require the consideration of geometric

factors between the targets and beam monitors:

$$\Phi_T = \kappa \frac{Y_{\rm BM}(E_n)}{\sigma_{\rm BM}(E_n)}. \quad (1)$$

In order to determine κ, the capture yield of a well-studied nucleus is measured and a scaling factor is determined to match the known cross section to the yield. The capture yield is related to the cross section by the following equation:

$$Y_T(E_n) = N_T \sigma_T(E_n) \Phi_T(E_n). \quad (2)$$

A 5-kÅ-thick ^{197}Au target was used for this procedure as it has a large capture resonance of approximately 26 kilobarns at a neutron energy of about 4.9 eV [13]. The 5-kÅ thickness minimizes the effects of multiple interactions and saturation effects. Additionally, the total cross section of ^{197}Au in this neutron energy region is dominated by neutron capture (≈90% of total cross section [13]), which simplifies the background subtraction. Reference [14] details how to account for the background in this measurement.

C. Detector efficiency

Since only a fraction of events are considered in the analysis, the percentage of events in the E_Σ and $M_{\rm cl}$ gates must be determined. To determine this efficiency, DANCE's response to γ cascades was simulated and the fraction of events that were excluded by the data cuts were calculated from the simulations. The simulations were based on a combination of DICEBOX code [15] γ-cascade generation and simulations of detector response in GEANT4 [16].

Several different models of photon strength functions (PSFs) and nuclear level density (NLD) for the theoretical inputs to DICEBOX were examined. They included PSF models based on generalized Lorentzian [17,18] and modified generalized Lorentzian (MGLO) [19] for $E1$ PSF and spin flip (SF), single-particle (SP) models, as well as a low-energy enhancement observed in many nuclei with the Oslo method [20] for $M1$ PSF. The constant-temperature (CT) and back-shifted Fermi gas model was then used for NLD. Models for DICEBOX simulation were validated via comparison to experimental spectra of multiplicity distribution, γ-ray energy distribution, and E_Σ distribution for different multiplicities. Here only the E_Σ distributions are shown.

Spectra of four resonances (likely with different spin and parity) for individual $M_{\rm cl}$ of ^{72}Ge are shown in Fig. 3. They were normalized to the same number of counts and are compared with simulations from $1/2^+$ resonances. Very similar PSFs and NLD models provide satisfactory description of spectra for ^{70}Ge as well. The simulated corridor (mean plus/minus one standard deviation) comes from different artificial nuclei produced in DICEBOX calculations normalized in the same way as experimental spectra. The simulated spectra show a spread comparable to that from experiment. In addition, the predictions for resonances with different spins and parities appear to be similar. This behavior implies that an efficiency for detection of events with $2 \leqslant M_{\rm cl} \leqslant 5$ and a range of E_Σ should be very similar for resonances with all relevant spins and parities.

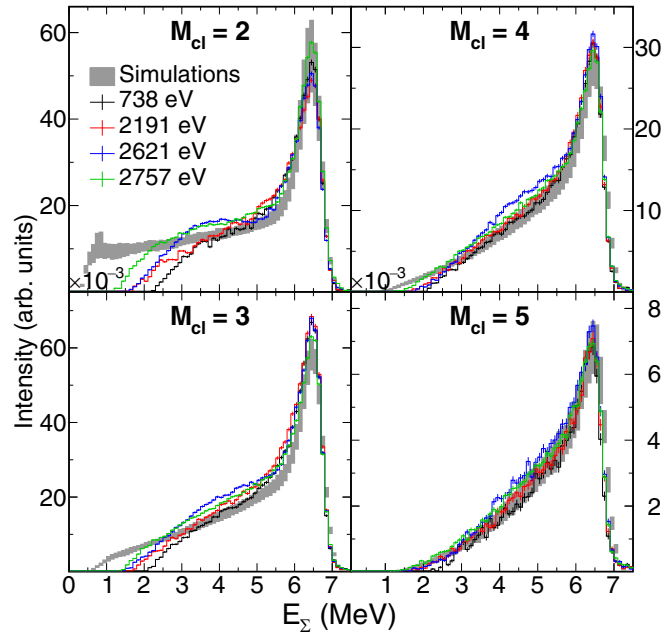

FIG. 3. A comparison of DANCE's simulated response (gray) with data from four different neutron resonances, specified in legend, for ^{72}Ge. Simulations were performed using MGLO model of $E1$ PSF, SF+SP combination in $M1$ PSF in conjunction with CT NLD model.

The fraction of events, $\varepsilon_{\rm cut}$, that occur within the multiplicity and E_Σ gates as a function of lower E_Σ limit, $E_\Sigma^{\rm min}$, for both Ge nuclei and s- and p-wave resonances is shown in Fig. 4. The limit for actual cross section analysis has been chosen to consider relatively broad range of E_Σ, which increases the statistical precision while constraining the uncertainty in the efficiency. Namely, $E_\Sigma^{\rm min} = 5.5$ and 4.5 MeV were considered for ^{70,72}Ge, respectively. The resulting efficiency values are $\varepsilon_{\rm cut} = 50.5 \pm 1({\rm stat.}) \pm 3({\rm sys.})\%$ and $57.4 \pm 0.5({\rm stat.}) \pm 3({\rm sys.})\%$ for ^{70}Ge and ^{72}Ge, respectively. Systematic uncertainties originate from variation between simulation and experimental data according to Ref. [21].

IV. RESULTS

A. Differential cross sections

Using the thin target approximation, the neutron capture cross section is given by:

$$\sigma_{n,\gamma} = \frac{Y_{n,\gamma}(E_n)}{\varepsilon_{\rm cut} f_a N_{\rm Ge} \Phi_T(E_n)}, \quad (3)$$

where $Y_{n,\gamma}$ is the background-subtracted capture yield, $N_{\rm Ge}$ is the number of atoms in the sample, and f_a is a target correction for neutron transmission to the beam monitors calculated using the total cross section from the Evaluated Nuclear Data Files (ENDF/B-VIII.0) database [13]. f_a deviates from unity only at the strongest resonances. Table III details the systematic uncertainties considered in these measurements.

Figure 5 shows a comparison of the cross section of ^{70}Ge measured in this work to the evaluated cross section in the ENDF/B-VIII.0 database. A number of resonances that were

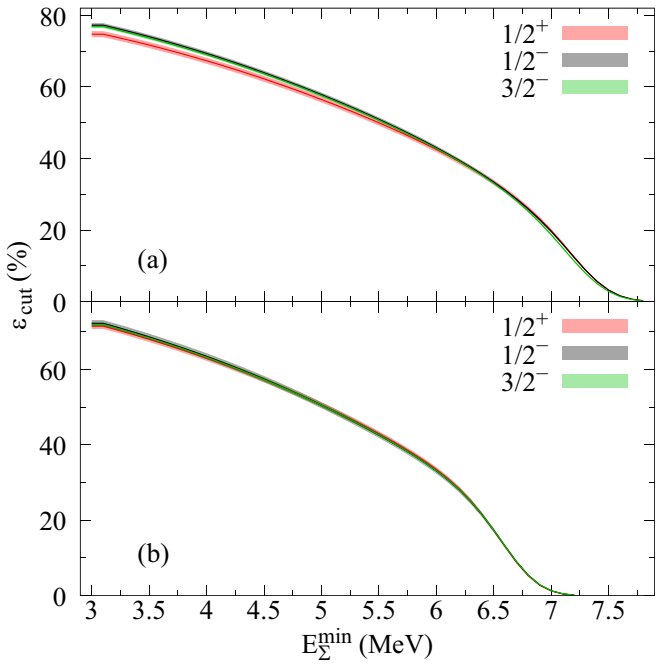

FIG. 4. Efficiency for detecting a γ cascade from neutron capture with $2 \leqslant M_{cl} \leqslant 5$ as a function of E_Σ^{min} for (a) ^{70}Ge and (b) ^{72}Ge. The 1σ bounds from the simulation of each line are given by shaded bands.

not identified in the evaluated cross section can be seen. This is also the first measurement of the cross section above 300 keV.

The energy differential cross section for ^{72}Ge was calculated in the same manner and is also shown in Fig. 5. As was the case with ^{70}Ge, several resonances that were not included in the evaluated cross section in the ENDF/B-VIII.0 database are present in the data. Most notably for astrophysics, a large capture resonance is seen at a neutron energy of approximately 6 keV in addition to smaller resonances below 10 keV. Because this region is close in energy to the astrophysically relevant region, the newly identified resonances have an effect on the stellar nucleosynthesis reaction rates predicted by the evaluated cross section. These resonances are also identified by the n_TOF collaboration.

TABLE III. Sources of systematic uncertainties considered in these measurements. Lightface values constitute sources of error in neutron fluence determination. Boldface values are added in quadrature to arrive at the total systematic uncertainty.

Source of uncertainty	1σ uncertainty (%)
Number of ^{197}Au atoms	4.0
κ fit	4.4
^{197}Au cross section	2.7
Neutron fluence	**5.9**
^{70}Ge efficiency	**7.9**
^{72}Ge efficiency	**6.1**
Number of Ge atoms	**0.2**
^{70}Ge total	**9.9**
^{72}Ge total	**8.5**

TABLE IV. ^{70}Ge MACS values from this work compared to those from the ENDF/B-VIII.0 and KADoNiS-v1.0 databases.

kT	MACS (mb)		
(keV)	This work	ENDF/B-VIII.0	KADoNiS-v1.0
5	196 ± 15	208 ± 62	207.3
10	147 ± 14	155 ± 39	154.8
20	107 ± 13	110 ± 17	109.8
30	89 ± 11	89 ± 5	89.1 ± 5.0
40	79 ± 10	77 ± 7	77.1
50	72 ± 9	70 ± 8	69.3
60	67 ± 8	64 ± 10	63.7
70	64 ± 8	60 ± 12	
80	61 ± 8	56 ± 13	56.2
90	59 ± 7	54 ± 14	53.1
100	57 ± 7	52 ± 16	51.4

B. Maxwellian-averaged cross sections

Because the energy of neutrons in a stellar environment is described by a Maxwell-Boltzmann distribution dependent on temperature, the Maxwellian-averaged cross sections (MACS) for each isotope were calculated as a function of kT using the following equation:

$$\sigma^{\mathrm{MACS}}(kT) = \frac{2}{\sqrt{\pi}} \frac{1}{(kT)^2} \int_0^\infty \sigma(E_n) E_n e^{-E_n/kT} dE_n$$
$$\approx \frac{2}{\sqrt{\pi}} \frac{1}{(kT)^2} \sum_a^b \sigma_{E_n} E_n e^{-E_n/kT} \delta E_n. \quad (4)$$

The integral is approximated by a discrete sum where the 0 to ∞ energy limits are replaced with the experimental limits $a = 10$ eV to $b = 1$ MeV. The neutron energy binning is logarithmic in order to avoid uncertainties due to the exponential dependence of the reaction rate on neutron energy.

MACS values were calculated for ^{70,72}Ge using the differential cross sections that were measured with DANCE. Note that the full neutron energy range needed to calculate these values was measured in this work, removing any reliance on external data or calculations. Tables IV and V show comparisons of the values from this work to two databases: ENDF/B-VIII.0 and Karlsruhe Astrophysical Database of Nucleosynthesis in Stars (KADoNiS-v1.0) [22].

C. Comparisons with recent measurements

Measurements of the neutron capture cross sections of ^{70}Ge and ^{72}Ge were recently published by Gawlik *et al.* [7] and Dietz *et al.* [8], respectively. These measurements were performed by the n_TOF collaboration at EAR-1 of n_TOF facility at CERN. A key difference between the n_TOF experiment and this measurement at the LANSCE facility is the detector setup, which leads to different data analysis methods.

Since DANCE is a 4π calorimeter, a measurement of the neutron capture cross section by means of directly subtracting

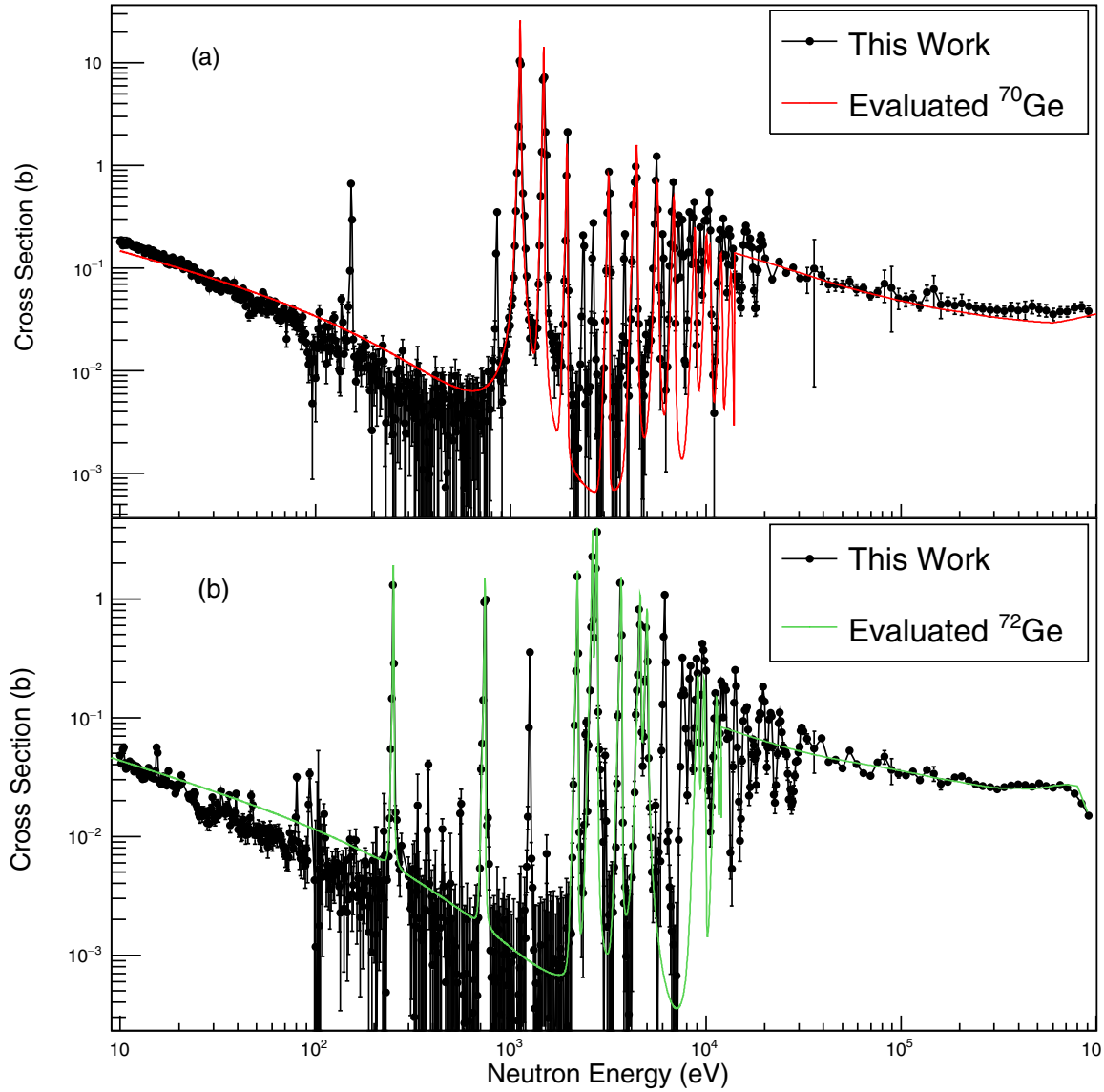

FIG. 5. Comparisons of the neutron capture cross sections of (a) ^{70}Ge and (b) ^{72}Ge with evaluated cross sections from the ENDF/B-VIII.0 database.

TABLE V. ^{72}Ge MACS values from this work compared to those from the ENDF/B-VIII.0 and KADoNiS-v1.0 databases.

kT	MACS (mb)		
(keV)	This work	ENDF/B-VIII.0	KADoNiS-v1.0
5	141 ± 10	102 ± 26	104 ± 26
10	102 ± 8	76 ± 19	80 ± 20
20	71 ± 6	61	67 ± 17
30	58 ± 5	53	59 ± 15
40	51 ± 5	49	54 ± 14
50	46 ± 4	45	50 ± 13
60	43 ± 4	43	47 ± 12
70	41 ± 4	41	
80	39 ± 4	39	43 ± 11
90	38 ± 4	38	
100	37 ± 3	37	40 ± 10

all backgrounds and impurities while having a good control of each contribution by measuring γ cascades can be performed. The n_TOF setup, on the other hand, employs a comparatively smaller array of four deuterated benzene (C_6D_6) detectors which are relatively insensitive to detecting scattered neutrons [23]. Capture yields are deduced using the total energy detection principle [24] in combination with the pulse-height weighting technique [25]. Additionally, n_TOF's comparatively longer flight path produces enhanced neutron energy resolution. The technique employed at n_TOF and the one from this work using DANCE thus complement one another. Complementary techniques are valuable for challenging capture cross-section measurements in this region of the chart of nuclides.

For ^{70}Ge, Fig. 6 shows a comparison of the results of this work with the recent measurement by Gawlik *et al.* [7], the older TOF measurement by Walter *et al.* [9], and the values from ENDF/B-VIII.0. The measurement from this work

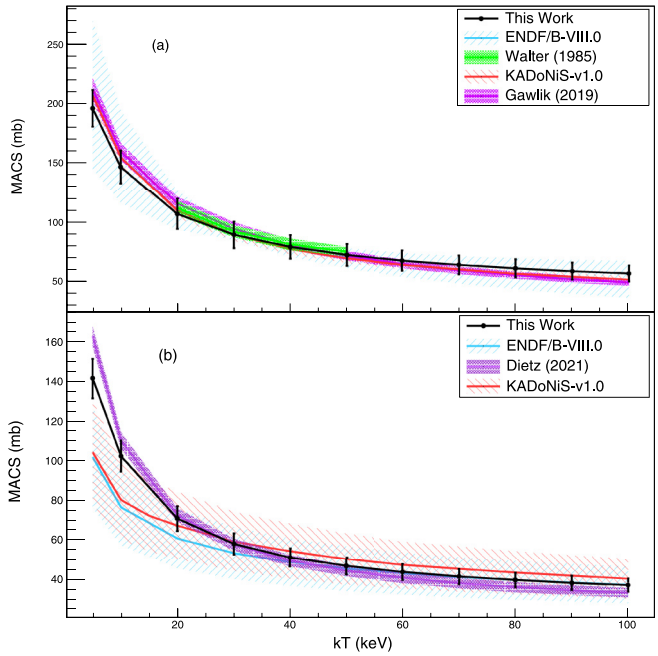

FIG. 6. Comparisons of the MACS from this work with previous measurements and evaluated database values for (a) ^{70}Ge and (b) ^{72}Ge.

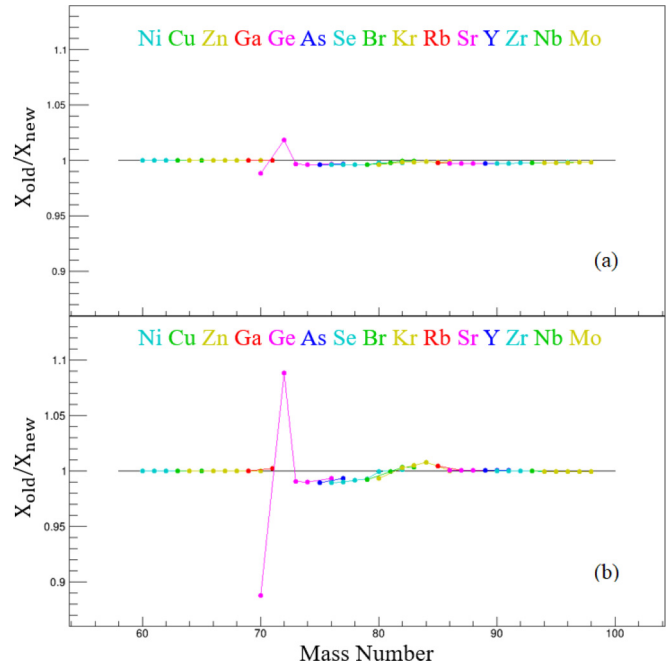

FIG. 7. A ratio of the NETZ weak s-process simulation results at (a) $kT = 30$ keV and (b) $kT = 90$ keV when including this work's measurements. Points are color coded according to elements and appear in order from lightest to heaviest.

shows good agreement ($<1\sigma$) with both experimental measurements as well as the database values. There is a slight divergence in the energy dependence at higher energies.

Figure 6 also shows a comparison of the ^{72}Ge MACS values from this work with Dietz *et al.* [8], and the values from the two databases. The measurement from this work is within 1σ agreement with the n_TOF measurement across the energy range studied with the exception of $kT = 5$ keV. According to both TOF measurements, the databases underestimate the MACS below approximately $kT = 30$ keV. Additionally, the measurement from this work shows excellent agreement with the ENDF database values above $kT = 50$ keV.

V. ASTROPHYSICAL IMPACT

MACS values have a direct influence on stellar nucleosynthesis reaction rates, and in the weak s process the effects on the reaction rate of one isotope propagate to isotopic abundances further along the s-process path. In order to assess the astrophysical effects of these measurements, the MACS values measured in this work were used in an s-process simulation network, NETZ [26]. NETZ is an online tool that allows the database reaction rate of any s-process isotope to be adjusted by a scaling factor and gives an output of the corresponding fractional change in isotopic abundances for all s-process isotopes. NETZ uses the KADoNiS-v1.0 database as a reference for MACS values.

Figure 7 shows a comparison of the changes in s-process abundances when including both measurements from this work for the two astrophysically relevant temperatures ($kT = 30$ and $kT = 90$ keV). The greatest change occurs in carbon shell burning where the abundance of ^{70,72}Ge are decreased and increased by about 10%, respectively. The abundance effects are less substantial for helium core burning where MACS from this work show more agreement with the database values.

At both temperatures, there is only minor change in downstream abundances when updated cross sections are included for both isotopes. For the case of helium core burning ($kT = 30$ keV), the measured ^{70}Ge cross section has good agreement with the KADoNiS values so there is little compounding effect between the two measurements. As for carbon shell burning ($kT = 90$ keV), the KADoNiS database underestimates the cross section of ^{70}Ge and overestimates the cross section of ^{72}Ge. There is a compensating effect between the two and the net result is a minor alteration ($<2\%$) in the weak s-process abundance for heavier isotopes.

VI. CONCLUSIONS

The neutron-capture cross sections of ^{70,72}Ge as a function of neutron energy were measured at LANSCE via the time-of-flight method using DANCE. The energy range for these measurements was 10 eV to 1 MeV, constituting the first measurement of the cross section for both isotopes above 300 keV. MACS in the astrophysically relevant energy range were extracted for each isotope. While the MACS for both ^{70}Ge and ^{72}Ge in this work exhibit substantial overlap with the n_TOF measurements, there are notable differences in the temperature dependence. Stellar nucleosynthesis calculations were performed using the NETZ code to examine the impact of these measurements on weak s-process abundances. While the abundances of ^{70,72}Ge are changed by up to 10%, the down-

stream effects are more subdued because of compensatory effects, namely that an increase in the cross section for ^{70}Ge is offset by a decrease in the ^{72}Ge cross section particularly at $kT = 90$ keV. This work also formed the basis for the graduate thesis of the first author. For more in-depth discussion of the data analysis, refer to Ref. [27].

ACKNOWLEDGMENTS

We would like to thank the beam operators at LANSCE for high-quality proton beams that were necessary for producing the neutrons. This research used resources of LANL's LANSCE facility, which is a DOE NNSA Designated User Facility operated by TRIAD National Security for the National Nuclear Security Administration of the U.S. Department of Energy (Contract No. 89233218CNA000001) and was supported by the USDOE under Grant No. DE-FG02-96ER40978. A. Couture, J. L. Ullmann, S. Mosby, and C. Prokop were supported by the U.S. Department of Energy through the Los Alamos National Laboratory. Support by the Grant No. 19-14048S of the Czech Science Foundation and the Charles University Project No. UNCE/SCI/013 is also acknowledged.

[1] E. M. Burbidge, G. R. Burbidge, W. A. Fowler, and F. Hoyle, Synthesis of the elements in stars, Rev. Mod. Phys. **29**, 547 (1957).

[2] D. Clayton, W. Fowler, T. Hull, and B. Zimmerman, Neutron capture chains in heavy element synthesis, Ann. Phys. **12**, 331 (1961).

[3] P. A. Seeger, W. A. Fowler, and D. D. Clayton, Nucleosynthesis of heavy elements by neutron capture, Ap. J. Suppl. **97**, 121 (1965).

[4] M. Heil, F. Käppeler, E. Uberseder, R. Gallino, and M. Pignatari, Neutron capture cross sections for the weak *s* process in massive stars, Phys. Rev. C **77**, 015808 (2008).

[5] M. Pignatari, R. Gallino, M. Heil, M. Wiescher, F. KÃ¤ppeler, F. Herwig, and S. Bisterzo, The weak s-process in massive stars and its dependence on the neutron capture cross sections, Astrophys. J. **710**, 1557 (2010).

[6] F. Kaeppeler, H. Beer, K. Wisshak, D. D. Clayton, R. L. Macklin, and R. A. Ward, s-process studies in the light of new experimental cross sections: Distribution of neutron fluences and r-process residuals, Astrophys. J. **257**, 821 (1982).

[7] A. Gawlik, C. Lederer-Woods, J. Andrzejewski, U. Battino, P. Ferreira, F. Gunsing, S. Heinitz, M. Krtička, C. Massimi, F. Mingrone *et al.* (n_TOF Collaboration), Measurement of the ^{70}Ge(n,γ) cross section up to 300 keV at the CERN n_TOF facility, Phys. Rev. C **100**, 045804 (2019).

[8] M. Dietz, C. Lederer-Woods, A. Tattersall, U. Battino, F. Gunsing, S. Heinitz, M. Krtička, J. Lerendegui-Marco, R. Reifarth, S. Valenta *et al.* (n_TOF Collaboration), Measurement of the ^{72}Ge(n,γ) cross section over a wide neutron energy range at the CERN n_TOF facility, Phys. Rev. C **103**, 045809 (2021).

[9] G. Walter and H. Beer, Measurement of neutron capture cross sections of s-only isotopes: Ge-70, Sr-86, and Sr-87, Astron. Astrophys. **142**, 268 (1985).

[10] K. Schoenberg and P. Lisowski, LANSCE, a key facility for national science and defense, Los Alamos Sci. **30**, 2 (2006).

[11] J. L. Ullmann, U. Agvaanluvsan, A. Alpizar, E. M. Bond, T. A. Bredeweg, E. Esch, C. M. Folden, U. Greife, R. Hatarik, R. C. Haight, D. C. Hoffman, L. Hunt, A. Kronenberg, J. M. ODonnell, R. Reifarth, R. S. Rundberg, J. M. Schwantes, D. D. Strottman, D. J. Vieira, J. B. Wilhelmy *et al.*, The detector for advanced neutron capture experiments: A 4π BaF_2 detector for neutron capture measurements at lansce, *International Conference on Nuclear Data for Science and Technology*, AIP Conf. Proc. No. 769 (AIP, Santa Fe, NM, 2005), p. 918.

[12] N. Abgrall, A. Abramov, N. Abrosimov, I. Abt, M. Agostini, M. Agartioglu, A. Ajjaq, S. I. Alvis, F. T. Avignone, III, X. Bai *et al.*, The large enriched germanium experiment for neutrinoless double beta decay (legend), *Workshop on Calculation of Double-Beta-Decay Matrix Elements (MEDEX'17)*, AIP Conf. Proc. No. 1894 (AIP, Prague, Czech Republic, 2017), p. 020027.

[13] D. A. Brown, M. B. Chadwick, R. Capote, A. C. Kahler, A. Trkov, M. W. Herman, A. A. Sonzogni, Y. Danon, A. D. Carlson, M. Dunn *et al.*, Endf/b-viii.0: The 8th major release of the nuclear reaction data library with cielo-project cross sections, new standards, and thermal scattering data, Nucl. Data Sheets **148**, 1 (2018) special Issue on Nuclear Reaction Data.

[14] C. J. Prokop, A. Couture, S. Jones, S. Mosby, G. Rusev, J. Ullmann, and M. Krtička, Measurement of the ^{65}Cu(n,γ) cross section using the detector for advanced neutron capture experiments at LANL, Phys. Rev. C **99**, 055809 (2019).

[15] F. Bečvář, Simulation of gamma cascades in complex nuclei with emphasis on assessment of uncertainties of cascade-related quantities, Nucl. Instrum. Methods Phys. Res., Sect. A **417**, 434 (1998); see erratum in Ref. [28].

[16] S. Agostinelli, J. Allison, K. Amako, J. Apostolakis, H. Araujo, P. Arce, M. Asai, D. Axen, S. Banerjee, G. Barrand *et al.*, GEANT4: A simulation toolkit, Nucl. Instrum. Methods Phys. Res., Sect. A **506**, 250 (2003).

[17] J. Kopecky, M. Uhl, and R. E. Chrien, Radiative strength in the compound nucleus ^{157}Gd, Phys. Rev. C **47**, 312 (1993).

[18] J. Kopecky and M. Uhl, Test of gamma-ray strength functions in nuclear reaction model calculations, Phys. Rev. C **41**, 1941 (1990).

[19] J. Kroll, B. Baramsai, G. E. Mitchell, U. Agvaanluvsan, F. Bečvář, T. A. Bredeweg, A. Chyzh, A. Couture, D. Dashdorj, R. C. Haight, M. Jandel, A. L. Keksis, M. Krtička, J. M. O'Donnell, W. Parker, R. S. Rundberg, J. L. Ullmann, S. Valenta, D. J. Vieira, C. Walker *et al.*, Strength of the scissors mode in odd-mass Gd isotopes from the radiative capture of resonance neutrons, Phys. Rev. C **88**, 034317 (2013).

[20] J. Rekstad, A. Henriquez, F. Ingebretsen, G. Midttun, B. Skaali, R. Øyan, J. Wikne, T. Engeland, T. F. Thorsteinsen, E. Hammaren, and E. Liukkonen, A study of the nuclear structure at high energy and low spin, Phys. Scr. T **5**, 45 (1983).

[21] M. Jandel, T. Bredeweg, A. Couture, M. Fowler, E. Bond, M. Chadwick, R. Clement, E.-I. Esch, J. ODonnell, R. Reifarth, R.

Rundberg, J. Ullmann, D. Vieira, J. Wilhelmy, J. Wouters, R. Macri, C. Wu, and J. Becker, GEANT4 simulations of the dance array, Nucl. Instrum. Methods Phys. Res., Sect. B **261**, 1117 (2007).

[22] The Karlsruhe Astrophysical Database of Nucleosynthesis in Stars 1.0 (test version), online at https://exp-astro.de/kadonis1.0/ latest release KADoNiS-0.3; I. Dillmann, M. Heil, F. Käppeler, R. Plag, T.Rauscher, and F. K. Thielemann, in *Capture Gamma-Ray Spectroscopy and Related Topics: 12th International Symposium, September 2005, Notre Dame*, edited by A. Woehr and A. Aprahamian (AIP, 2006), p. 123.

[23] R. Plag, M. Heil, F. Käppeler, P. Pavlopoulos, R. Reifarth, K. Wisshak (n_TOF collaboration), An optimized C_6D_6 detector for studies of resonance-dominated (n, γ) cross-sections, Nucl. Instrum. Methods Phys. Res., Sect. A **496**, 425 (2003).

[24] R. L. Macklin and J. H. Gibbons, Capture-cross-section studies for 30220-keV neutrons using a new technique, Phys. Rev. **159**, 1007 (1967).

[25] U. Abbondanno, G. Aerts, H. Alvarez, S. Andriamonje, A. Angelopoulos, P. Assimakopoulos, C. O. Bacri, G. Badurek, P. Baumann, F. Bečvár *et al.* (n_TOF collaboration), New experimental validation of the pulse height weighting technique for capture cross-section measurements, Nucl. Instrum. Methods Phys. Res., Sect. A **521**, 454 (2004).

[26] M. Weigand, T. A. Bredeweg, A. Couture, K. Göbel, T. Heftrich, M. Jandel, F. Käppeler, C. Lederer, N. Kivel, G. Korschinek, M. Krtička, J. M. O'Donnell, J. Ostermöller, R. Plag, R. Reifarth, D. Schumann, J. L. Ullmann, and A. Wallner, ^{63}Ni(n, γ) cross sections measured with DANCE, Phys. Rev. C **92**, 045810 (2015).

[27] A. Laminack, Stellar nucleosynthesis: Direct measurement of the neutron-capture cross sections of stable germanium isotopes and design of a next generation ion trap for the study of β-delayed neutron emission, LSU Doctoral Dissertations, Louisiana State University, Baton Rouge, Louisiana, 2020.

[28] F. Bečvář, Erratum to "Simulation of gamma cascades in complex nuclei with emphasis on assessment of uncertainties of cascade-related quantities [Nucl. Instrum. Methods A 417 (1998) 434–449]," Nucl. Instrum. Methods Phys. Res., Sect. A **935**, 240 (2019).